A Structural Shape based Palmprint Recognition

[1][*]Zanobya N. Khan, [2]Jamil Ahmad, [3]Zahoor Jan, [4]Hamid Jan

[*1,4] *Department of CS & IT, Sarhad University of Science and It, Peshawar-Pakistan,*
zanoby.nisar@gmail.com, engrhamidjan@yahoo.com
[2,3]*Islamia College Peshawar (Chartered University), Peshawar-Pakistan,*
jamil.ahmad.icp.edu.pk, zahoor.jan@icp.edu.pk

Abstract

In this article, for finding an efficient Palmprint Recognition (PPR) system, three different methods for palmprint recognition system are compared. We adopted Niblack binarization method for the extraction of line features in palmprint followed by their endpoints detection. The endpoints of these lines are then utilized in the construction of three most important members of the polygons; Delaunay Triangulation (DT), Convex Hull (CH) and Irregular Polygon (IP). These polygons are then incorporated with quantitative and geometric features as well as some important shape descriptors. Finally, machine learning algorithms including Naïve Bayes, Random forest, Multilayer perceptron, K-nearest neighbor and weighed sum are used to ascertain the performance of the methods discussed in this manuscript. This extensive analysis will benefit the selection and adoption of appropriate methods for the concerned needs of the users for PPR.

Keywords: Polygons, Naïve Bayes, Multilayer Perceptron, Learning theory, Palmprint recognition

1. Introduction

Palmprint, an inner surface of the hand, consists of wide thick lines (principal lines), thin irregular lines (wrinkles), and texture, minutiae, palm-vein and delta points. These features can be extorted at different resolutions. Palm line features including principal lines and wrinkles offers stability, reliability and individuality. Thus, a successful and accurate palmprint recognition system can be designed using the significant palm line features. Palm lines have greater visibility and can be extracted even from low resolution images [1]. Moreover, these images can also be captured using low-priced devices such as digital and video cameras. In addition to the line features, palmprint is encompassed with certain geometric features such as length, area, width and perimeter of a palm. However, the practical applicability of geometry features is limited to small size database with a high probability of being faked easily [2].

Bouchemha et al. [3] adopted DT for the representation of palmprint principal lines and used Hausdorff distance as a classifier whereas A. Kumar et al. [4] performed triangulation of hand veins. DT approach has produced promising results for fingerprint and face recognition, however, none of the prior work used CH and IP for PPR. Further, the applications of DT and CH can be found in various fields such as computer vision, pattern recognition, image processing, robotics and computational geometry. Therefore, in this article, taking PPR as an application scenario, we conduct a series of experiments to investigate the DT, IP and CH for PPR. We have extracted different set of features such as quantitative, geometric and some important shape descriptors from DT, IP and CH constructed using the endpoints of palm lines detected. The quantitative features analyze DT, IP and CH quantitatively whereas shape descriptors are extracted from the shape of the CH and IP only. To further add viability and discriminability, geometric features are attributed to the edges of the CH, IP and triangles of the DT. All these forms a feature vector which are subsequently used in the creation of our palmprint model. We have used machine learning classifiers namely Naïve Bayes, Random Forest, Multilayer

Perceptron (MLP), k-nearest neighbor (K-NN) and weighted sum for evaluating the performance of the three proposed techniques. We have selected these classifiers based on their performance in the Computer Vision research and the state-of-the-art. The flow diagram of the proposed technique is given in Figure 1.

In Section 2, we review the previous work in PPR. In Section 3, proposed line extraction technique is described and set of features extracted from the polygons is discuss in Section 4. Section 5 presents experimental evaluation of classification accuracy using various machine learning algorithms as well as a weighted sum model.

2. Related Works

In [5], Huang et al. propose modified finite radon transform and a dynamic threshold to extract wrinkles and principal lines. In the matching phase, similarity between two palmprint is computed using pixel-to-area based algorithm. In [6], Wu et al. extract palm lines in two stages: coarse level and fine level. At the course level, principal lines and wrinkles are extracted using morphological operators and line directional masks. At the fine level, for each extracted line recursive processes is applied to further extract and trace any missing parts of the palm line. Wong et al. [7] employ Sobel masks of two sizes (3x3 and 5x5) to extract principal lines and used Hamming distance as a classifier. Jayoti et al. [8] extracted line features including principal lines, wrinkles and ridges using phase congruency edge detector in six different orientations. Hamming distance with sliding window is use to compare two feature vectors. Anhui et al. [9] propose hierarchical palmprint matching. First, line edge map (LEM) of palmprint is extracted and then line based Hough Transform is applied to extract global features for coarse level matching. In the fine level matching, local features such as position, orientation of individual lines are extracted. Line based Hausdorff (LDH) distance is used for matching. Bouchemha [4] extracted principal lines using line directional mask. Radon Transform and adaptive thresholding is then applied to extract maximum coefficients along each projection from which centroids are extracted. These centroids are connected to each other by means of Delaunay triangulation and matched using Hausdorff distance. The Delaunay triangulation has been used widely for fingerprint and face recognition. G. Behis [10] proposed fingerprint identification system using Delaunay triangles for indexing. This reduced the memory requirements without compromising the recognition accuracy and persevered similarity without restoring to high dimensional indexing. In [11], Ning Liu used DT for fingerprint matching and developed a matching algorithm based on DT Net to find reference minutiae pairs.
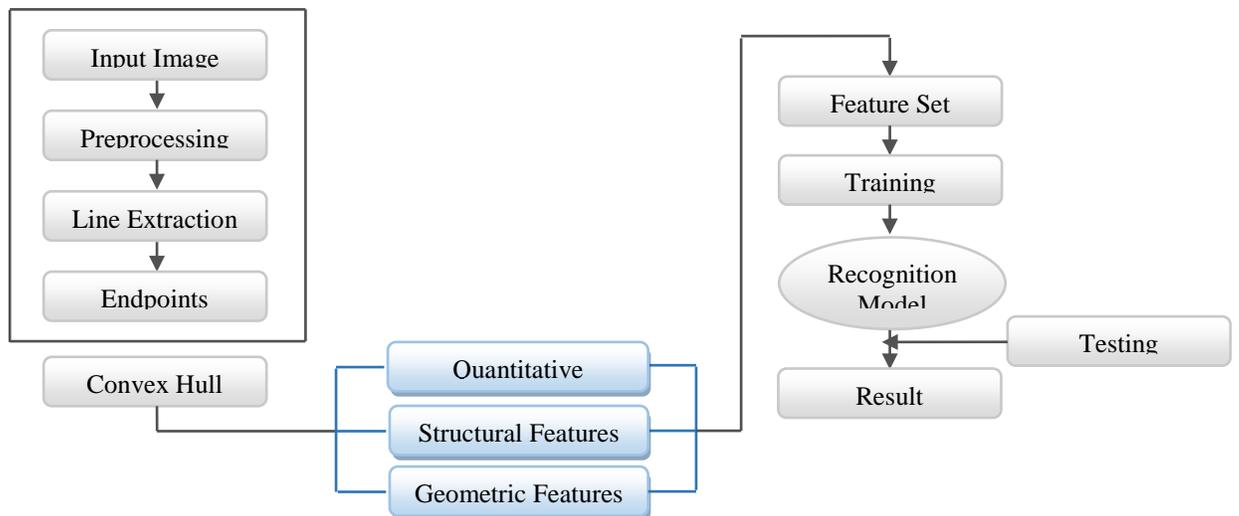

Figure 1. Flow diagram of the proposed approach

3. Palm Lines Detection

The palm lines comprise of both principal lines and wrinkles. In order to extract these line features, initially the input palmprint image is smoothed using median filter and morphological opening. Instead of using edge detection techniques, we exploited Niblack binarization method to extract lines [12-13]. This proposed method proved relatively effective in extracting the whole line; however, most of the state of the art approaches in the literature also successfully extracted these lines but not a complete line. Further processing involves area thresholding, closing and thinning. Finally, from single pixel thick lines, endpoints for all the palm lines are then determined as depicted in Figure. 2.
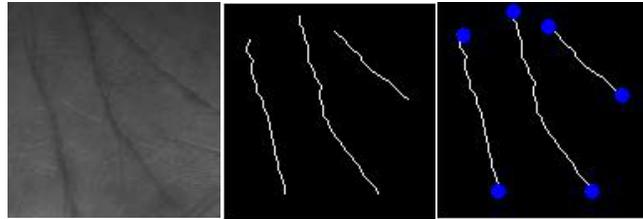

Figure 2. Detection of palm lines from their endpoints

4. Palmprint Features

The most commonly used members of polygon family are exploited including CH, IP and DT for effective representation of palmprints. Both are constructed utilizing the endpoints of all palm lines. The CH from lines endpoints is created as shown in Figure. 3 using the algorithm in [14].We then extracted different features from the CH that includes quantitative which includes total number of CH edges and endpoints of lines, shape descriptors and geometric thus forming a feature vector.
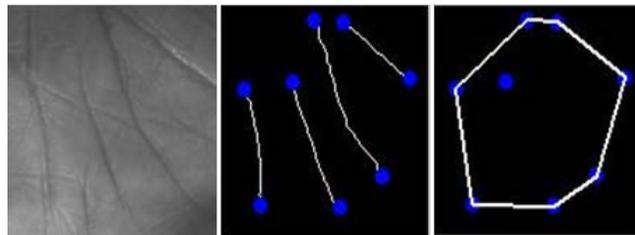

Figure 3. Convex hull created from lines endpoints

4.1 Convex Hull based Features

The shape of the CH can be described by using some of the important shape properties illustrated in Table 1. These features have been selected such that they can prove helpful in defining and characterizing the CH shape. Another important shape property used to define the shape of a CH is the Hu [15] invariant moments. However, only the first four moments are used to distinguish the CH since the remaining moments have insignificant effect in enhancing the performance.

Table 1. Shape Features

Feature	Description
Rectangularity	Ratio of the area of convex hull to area of minimum bounding rectangle
Circularity	Ratio of area of convex hull to its squared perimeter
Solidity	Proportion of the pixels of convex hull that are also in the region
Elongation	Ratio of the width and length of the minimum bounding angle of the shape
Orientation	Angle between x-axis and major axis of the ellipse
Centroids	Specifies the center of the convex hull
Major axis length	Length of major axis of ellipse that has same normalized second central moments as the region
Minor axis length	Length of minor axis of ellipse that has same normalized second central moments as the region

4.2 Geometric Features

The quantitative features and shape descriptors given in Table 1 can only discriminate CH shapes with large differences and are used for initial filtering purposes so as to assist in bringing the CH of similar shapes together present in the database. Nevertheless, the discriminability of the proposed approach is ensured by associating the edges of the CH with some important geometric features. These features play a vital role to discriminate palmprints that belongs to different classes and substantially improve the overall performance of the proposed approach. The geometric features comprise of area, perimeter, length and angles. The area of CH is defined as the total number of pixels within the whole CH region whereas perimeter is the count of the number of pixels around its boundary.

4.2.1 Length: Let $(\ell\varepsilon_1, \ell\varepsilon_2, \dots \ell\varepsilon_n)$ be the edges of a convex hull and (a_i, b_i) represent the coordinates of the respective endpoints. The length for each edge of the convex can then be computed as

$$\ell\varepsilon_i = \sqrt{\sum_{i=1}^{n}\left(\left(x_2(i) - x_1(i)\right)^2 + \left(y_2(i) - y_1(i)\right)^2\right)} \qquad (1)$$

The length features can be normalized by taking the ratio of the length of CH edge to the length of the edge with greatest value $(\ell\varepsilon_{max})$. The normalized lengths [16] determined are then assorted to five different classes and a range is specified for each class at an interval of 0.2 as tabulated in Table 2.

$$N\ell\varepsilon_i = {\ell\varepsilon_i}/{\ell\varepsilon_{max}} \qquad (2)$$

4.2.2 Angle: The orientation for each edge of the CH along horizontal axis can be calculated using the slope intercept form defined as

$$Slope(i) = \frac{(y_2(i) - y_1(i))}{(x_2(i) - x_1(i))} \qquad (3)$$

$$G\theta_i = \tan^{-1}(slope\ (i)) \qquad (4)$$

Since the edges of a CH makes angle with x-axis, its value therefore will always be between 0° and $180^°$. These values are also categorized into six different classes with an interval

Features	Range
$N\ell\mathcal{E}_1$	$0 \leq N\ell\mathcal{E}_1 \leq 0.2$
$N\ell\mathcal{E}_2$	$0.2 < N\ell\mathcal{E}_2 \leq 0.4$
$N\ell\mathcal{E}_3$	$0.4 < N\ell\mathcal{E}_3 \leq 0.6$
$N\ell\mathcal{E}_4$	$0.6 < N\ell E_4 \leq 0.8$
$N\ell\mathcal{E}_5$	$0.8 < N\ell\mathcal{E}_5 \leq 1.0$

Table 2. Normalized length features

Features	Range
$G\theta_1$	$0 \leq G\theta_1 \leq 30^°$
$G\theta_2$	$30^° < G\theta_2 \leq 60^°$
$G\theta_3$	$60^° < G\theta_3 \leq 90^°$
$G\theta_4$	$90^° < G\theta_4 \leq 120^°$
$G\theta_5$	$120^° < G\theta_5 \leq 150^°$
$G\theta_6$	$150^° < G\theta_6 \leq 180^°$

of 30° given in Table 3.

Table 3. Angular features

4.3 Irregular Polygon based Features

The In the proposed approach, the coordinates of the endpoints of the lines are also utilized in creating IP as given in Figure. 4. The features extracted from both the contour and interior of IP comprise of quantitative features, shape descriptors and geometric features. These features are the same as those determined from the shape of the CH and discussed in detail in 4.2.
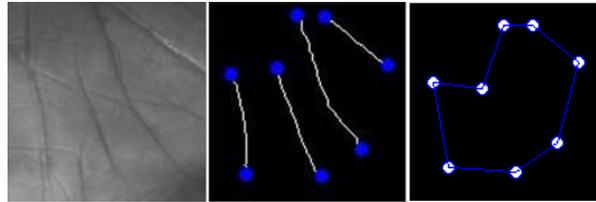

Figure 4. Irregular polygon constructed from endpoints of lines

4.4 Delaunay Triangulation based Features

The area of The DT of each palmprint is constructed using the coordinates of the endpoints of palm lines such that the circum-circle associated with each triangle does not contain a point in its interior as depicted in Figure. 5. The DT obtained for each of the palmprint is associated with features which are not only easy to compute but are also discriminant enough to differentiate between palmprint images. The quantitative features consist of number of triangles in triangulation and endpoints of lines. The DT associated with geometric features include relative length, surface area, angle and in-centers. However, relative length and angle for the vertices of triangles are computed and categorized into different classes in the same manner as discussed in 4.2 and given in Table 2 and Table 3 respectively. Nevertheless, relative area and in-center features are detailed below.
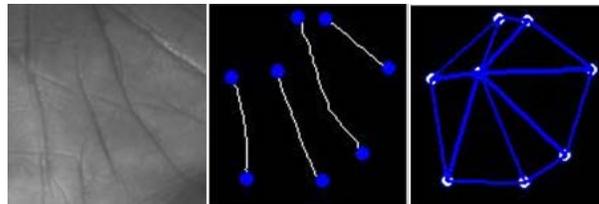

Figure 5. DT created from lines endpoints

4.4.1 Relative Area: The area of each of the independent triangle can be determined using the information available at the vertices of the triangles in the triangulation. The area of a triangle can be defined as half the product of base and its corresponding height.

$$A = \frac{1}{2}(bh) \tag{5}$$

The parameters of the area i.e. base and height can be obtained using the Pythagoras theorem. Nonetheless, relative areas (RA_i) are taken to ensure scale invariant property and then assorted to five different classes (see Table 3). It can be defined as

$$\mathcal{RA}_i = \frac{\mathcal{A}_i}{\mathcal{A}_{max}} \tag{6}$$

4.4.2 Relative In-centers: The in-center for every triangle in the DT is also computed and normalized by taking relative in-centers. The relative in-centers are also classified into different classes as tabulated in Table 3.

$$C\mathcal{A}_i = \frac{C_i}{C_{max}} \tag{7}$$

5. Experimental Setup and Result Analysis

The experiments are conducted on the publicly available 2D Palmprint ROI database collected by the Biometric Research Center of Hong Kong Polytechnic University. The effectiveness of the proposed approach is examined on a modest- sized dataset of 420 images that belongs to 70 different individuals. In our experiment, six images are randomly selected of each individual, among which five images are used for training and the remaining one image is used for testing. The feature vector of different palmprints obtained from the CH, IP and DT are evaluated using several machine learning algorithms such as Naïve Bayes, Random Forest, Multilayer Perceptron and K-nearest neighbor in addition to the weighted sum model.

5.1 Parameter Tuning in Classifiers

In order to acquire optimum results with minimum execution time, some of the main parameters in Naïve Bayes (NB), RF, MLP, K-NN and weighted sum are fine-tuned. The probabilities of numeric attributes in Naïve Bayes are computed using either the probability density function of normal distribution or kernel density estimation. However, we deduced from the experimental results that kernel density estimation fails to produce good result as compared to normal distribution. In random forest, the two most important parameters that have to be optimized are: Number of trees η_{tree} in the forest and a number of features selected randomly at each node. After experimenting with different values of trees, we set this parameter η_{tree} to 16 with OOB error also minimized. The number of features selected parameter is tuned using the default value suggested by Briemen [17] which is equal to square root of total number of features. In the proposed approach, we have a total of 28 features; square root of 28 is 5.2 and without rounding it off we choose the default value of 5 for number of features.

The performance of MLP neural network can be assessed by fine tuning some of the parameters that could have a positive impact on the classification accuracy. These include number of hidden layers and neurons, learning rate α and the momentum μ. In this manuscript, better performance is obtained with only one hidden layer having 30 nodes. Similarly, learning rate and momentum is set to 0.3 and 0.4 respectively.

The performance of MLP neural network can be assessed by fine tuning some of the parameters that could have a positive impact on the classification accuracy. These include number of hidden layers and

neurons, learning rate α and the momentum μ. In this manuscript, better performance is obtained with only one hidden layer having 30 nodes. Similarly, learning rate and momentum is set to 0.3 and 0.4 respectively.

   In k-nearest neighbor algorithm, an important parameter that influences the classification performance is the value of *k=1*, where *k* is the neighborhood size. In weighted sum model, the distance between the feature vectors is computed using the Sorensen [18] distance. The geometric features have been assigned higher weight as they are more discriminative as compared to other features. The Sorensen distance can be defined as:

$$Sd_{ij} = \frac{\sum_{k=1}^{n}|x_{ik} - x_{jk}|}{\sum_{k=1}^{n}(x_{ik}) + \sum_{k=1}^{n}(x_{jk})} \qquad (8)$$

5.2 Discussion

For performance evaluation, we use Classification Accuracy and F-measure.   The classification accuracy is calculated as follows:

$$Accuracy = \frac{Number\ of\ correctly\ classified\ images}{Total\ number\ of\ images} \times \qquad (9)$$

While for F-measure, we use the standard F-measure which is normally used for comparative analysis:

$$F-measure = 2 \times \frac{(precision \times recall)}{(precision + recall)} \qquad (10)$$

   For experimentation point of view, we denote CH approach as CHPPR, DT approach as DTPPR and IP approach as IPPPR. Figure 6 show that CHPPR representation of palmprint achieved best performance with NB by obtaining 98.33% classification accuracy as compared to 61.66% by DTPPR and 92.86 % by IPPPR. Moreover, with the MLP, CHPPR achieved 90% accuracy and decreased to 88.57% and 87.14% respectively for RF and K-NN. With, DTPPR no such improvement in performance can be seen when experiments are conducted with MLP (60% accuracy). When experiments are conducted with MLP, a slight decrease can be observed in the performance of IPPPR by acquiring 90% classification accuracy.

   The performance of K-NN with IPPPR and DTPPR has been worst and this may be due to the fact that it does not include any training phase. The results in Figure 6 shows a sudden decrease in the performance of CHPPR and IPPPR when experiments are conducted on weighted sum as its accuracy reduces to 81.66% and 82.85% respectively. On the other hand, the DTPPR failed to produce promising result on any of the classifier except the weighted sum model achieving 85% accuracy. Thus, it can be deduced from the experimental analysis that CHPPR approach outperforms DTPPR and IPPPR approaches.

   In addition to classification accuracy, it can also be analyzed from Figure 6 how the performance of several classifiers is affected by features. It is also interesting to note that with shape descriptors, a significant improvement in the performance of PPR can be observed. Therefore, promising results are achieved with CHPPR approach followed by IPPPR. However, with DTPPR even the use of some popular machine learning classifiers does not show substantial improvement in its performance.

   The Figure 7 shows with results using the reduced feature vector. A reduced feature vector consists of only quantitative and geometric features. Both CHPPR and IPPPR achieve 70% accuracy on RF and K-NN. Similarly, for the same feature vector, the DTPPR managed to produce somewhat better results by achieving an accuracy of 85% only when experiments are performed with weighted sum model whereas on other classifiers the performance is low.

   Figure 8   shows the F-measure (also tabulated in Table 4) which is a plot of precision and recall. In this Figure, the F-measure of NB with CHPPR DTPPR and IPPPR based features is 0.98, 0.55 and 0.91 respectively. The Fig. 9 depicts that CHPPR give 43% better performance than DTPPR and 7%

than IPPPR with NB. Furthermore, the F-measure shows that there is no substantial improvement in the performance of DTPPR in comparison with CHPPR and IPPPR. However, DTPPR obtained an F-measure of 0.81 with weighted sum whereas CHPPR and IPPPR F-measure is reduced to 0.76 from 0.98 and from 0.77 to 0.91. This reduction in the performance can be visualized in a simple retrieval scenario depicted in Figure 9.

Also Figure 9 shows samples of some of the images which the DTPPR approach failed to recognize correctly. The images in Figure 9 (a) though belong to two different individuals have been classified as belonging to the same individual. This incorrect classification is due to the resemblance in their feature based structural triangulation. With reference to Figure 9(b), the shapes of the triangulation are quite different but due to same number of triangles, the two images of two different individuals are recognized incorrectly. In Figure 9(c), the similarity parameter among triangulation of palmprint images is considerably high and therefore incorrectly classified and recognized as belonging to the same individual.

Nevertheless, DT has been employed successfully for face and fingerprint recognition, however, in the proposed approach, the results obtained from the DTPPR are not satisfactory at all despite of using some important machine learning algorithms for identification. This can be attributed to the fact that the features extracted from the triangles of DT are generally discretized into various classes which can contain some redundant data. On the other hand, amalgamation of structural features with quantitative and geometric features and usage of state-of-the-art machine learning classifiers for CHPPR and IPPPR, the performance for these approaches has improved substantially. The CHPPR slightly outperforms the IPPPR due to the optimized structure obtained from the CHPPR. In the case of IPPPR, an outlier strongly affects the result. However, in the case of CHPPR, this effect is slightly reduced due to the well-developed representation of CH.
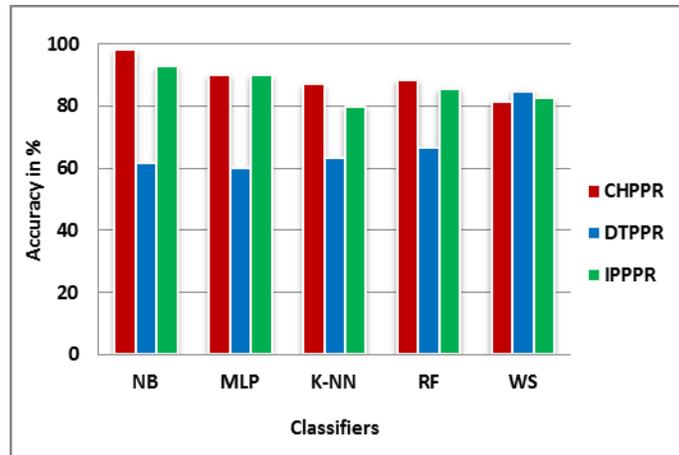

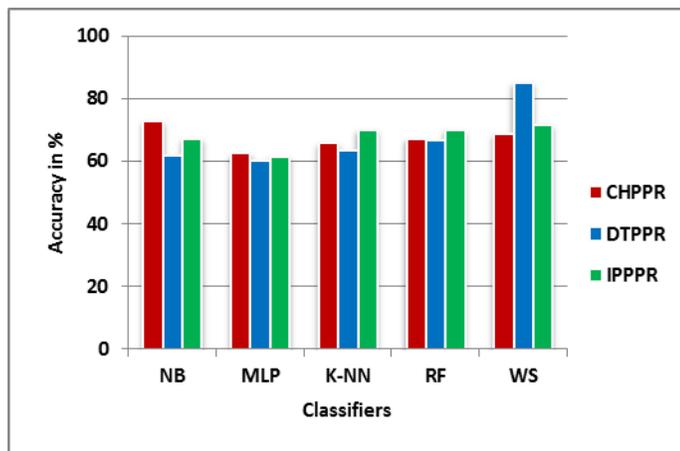**Figure 6.** Accuracy of proposed techniques using various classifiers

Figure 7. Per **Table 4.** Evaluation of proposed techniques in terms of F-measure   ccuracy

Classifiers	CHPPR	DTPPR	IPPPR
NB	0.98	0.55	0.91
MLP	0.86	0.51	0.88
K-NN	0.84	0.57	0.75
RF	0.85	0.59	0.81
WS	0.73	0.82	0.77

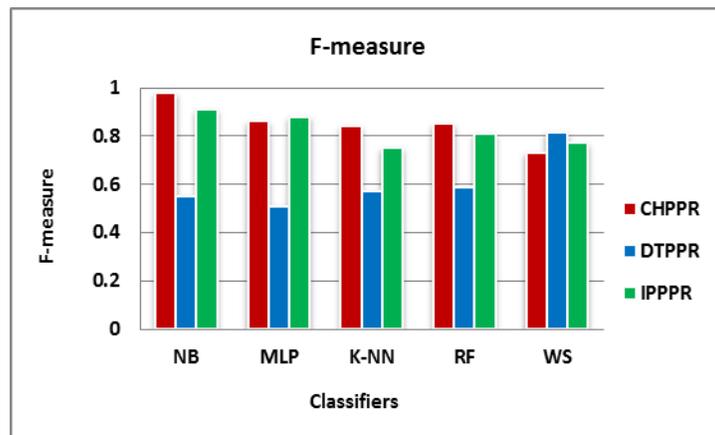**Figure 8.** F-measure of different classifiers for proposed approaches

(a)   (b)   (c)
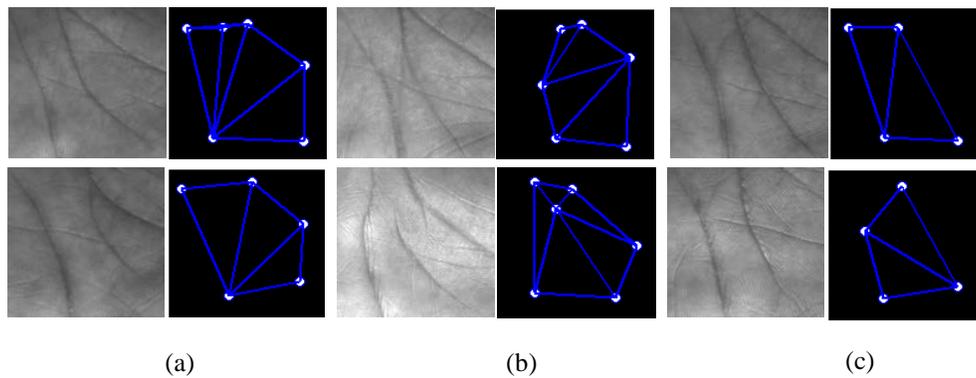
Figure 9. Palmprint images detected incorrectly by the DTPPR approach

5.3 Runtime Analysis

For the run-time analysis, we report the experiments based on core-i5 (2.6 GHz), having 4GB RAM in the MatLab environment to determine the effectiveness of the proposed approaches. The execution time for the palm line extraction, their endpoints including preprocessing and construction of CH (on average for a single image) is 0.37 seconds whereas the DTPPR approach took 0.42 seconds from the

extraction of line features to its construction. From Figure 10, it can be seen that the construction of IP from the endpoints of palm lines turns out to be quite time consuming. It is evident from the results given in Figure 10 that CHPPR approach is computationally more efficient.
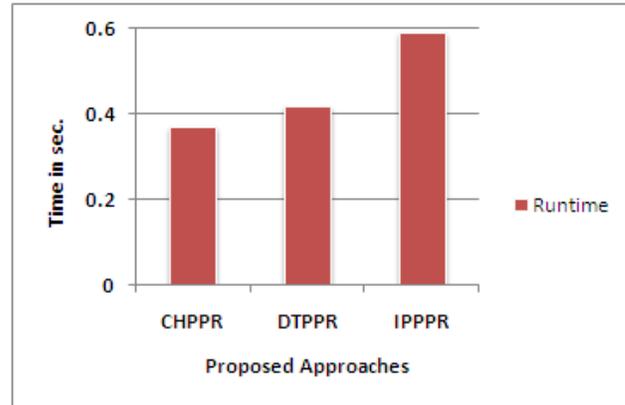

Figure 10. Runtime comparison of the proposed approach

6. Conclusion

For the palmprint recognition point of view, we analyzed the performance of three different methods i.e. CH, IP and DT. The CH, IP and DT are constructed from the endpoints of palm lines. These are associated with different set of distinct features. For justified analysis, the results are compared using the state-of-the-art Machine Learning Classifiers, Random Forest, MLP, KNN, Naïve Bayesian and Parametric approach the Weighted Sum. The extensive experimentation depicts that CH feature based approach with Naïve Bayes produced promising results and can be efficiently used for the design of a palmprint recognition system. Further, it is concluded that the use of an appropriate classifier can have a positive impact on the design and implementation of a successful biometric system.

7. References

[1] Zhou Guo, David Zhang, Lei Zhang and Wang Zuo, "Palmprint verification using binary orientation co-occurrence vector", Pattern Recognition Letters, vol. 30, no. 13, pp. 1219-1227, October 2007.
[2] Adam Kong, "Palmprint identification based on generalization of Iriscode". PhD, Waterloo University, Ontario, Canada, 2007.
[3] Amel Bouchemha, Amine Nait Ali and Doghmane, "A robust technique to characterize palmprint using radon transform and delaunay triangulation", Intl' J Computer Applications, vol. 10, no. 7, pp.35-42, 2010.
[4] Ajay Kumar and Prathyusha, "Personal authentication using hand vein triangulation and knuckle shape", IEEE Trans. on Image Processing, vol. 18, no. 9, pp. 2127-2136, September 2009.
[5] De-Shuang Huang, Wei Jia and David Zhang, "Palmprint verification based on principal lines". J Pattern Recognition, vol. 41, no. 28, pp. 1316-1328, April 2008.
[6] Xie Wu and Kia Wang, "A novel approach of palm line extraction", in Proc. of 1st IEEE Conf. on Image and Graphics Conference, pp. 230-233, December 18-20 2004.
[7] Kia Yih Edward Wong, Ali Chekima and Jamal Ahmad, "Palmprint identification using sobel operator", in Proc. of IEEE Conf. on Control, Automation, Robotics and Vision, pp. 1338-1341, December 17-20 2008..
[8] Jayoti Malik, Dahiya and Sainarayanan Gayatri, "Personal authentication using palmprint with phase congruency feature extraction method", Intl' J of Signal Processing, Image Processing and Pattern Recognition, vol. 4, no. 7, pp. 1313-1325, 2011.

[9] W.Anhui and N.Jiangsu, "Palmprint recognition using line edge map", Intl' J of Digital Content Technology and its Applications, vol. 6, no. 2, pp. 285-291, 2012.

[10] George Bebis, Deaconu T and Georgiopoulos G, "Fingerprint identification using delaunay triangulation", in Proc. of IEEE Conf. on Information Intelligence and Systems, pp. 452-459, Oct 31– 3 Nov 1999..

[11] Ning Liu, Yilong Yin and Hongwei Zhang, "A fingerprint matching algorithm based on delaunay triangulation net", in Proc. of IEEE Conf. on Computer and Information Technology , pp.591-595, September 21-23 2005.

[12] Zanobya Nisar, Zahoor Jan, Rehanullah Khan and R. J. Qureshi, "Palmprint recognition: A naïve bayesian approach", World Applied Sciences Journal, vol. 31, no. 11, 2014.

[13] Zanobya N. Khan, Rashid Jalal Qureshi and Jamil Ahmad, "On Feature based Delaunay Triangulation for Palmprint Recognition", Journal of Platform Technology, vol. 3, no. 4, December 2015.

[14] Maher, Atwah M and Johnnie W. Baker, "An associative dynamic convex hull algorithm", in Proc. of IASTED Conf. on Parallel and Distributed Computing Systems, pp. 1-5, February 15-17 1998.

[15] Ming Kuei Hu, "Visual pattern recognition by moment invariants", Information Theory, IRE Transactions, vol. 8, no. 2, 1962.

[16] Rashid Jalal Qureshi, Ramel, Cardot H and Prachi Mukherji, "Combination of symbolic and statistical features for symbols recognition", in. Proc. of IEEE Conf. on Signal Processing, Communication and Networking, pp. 477-482, February 22-24 2007.

[17] Leo Breiman, "Random Forest", J Machine Learning, vol. 45, no. 13, pp. 5-32, 2001.

[18] Micheal Michie, "Use of the bray-curtis similarity measure in cluster analysis of foraminiferal data", J of the Intl' Association for Mathematical Geology, vol. 14, no. 6, pp. 661-667, 1982.